Slow dynamics of electron glasses: The role of disorder

Z. Ovadyahu
Racah Institute of Physics, The Hebrew University, Jerusalem 91904, Israel
(Received 31 October 2016; revised manuscript received 31 January 2017; published 13 April 2017)

We examine in this work the role of disorder in contributing to the sluggish relaxation observed in intrinsic electron glasses. Our approach is guided by several empirical observations: First and foremost, Anderson localization is a pre-requisite for observing these nonequilibrium phenomena. Secondly, sluggish relaxation appears to favor Anderson insulators with relatively large Fermi energies (hence proportionally large disorder). These observations motivated us to consider a way to measure the underlying disorder in a realistic Anderson insulator. Optical studies using a series of amorphous indium oxide (In_xO) establish a simple connection between carrier concentration and the disorder necessary to approach the metal-insulator transition from the insulating side. This is used to estimate the typical magnitude of the quenched potential fluctuation in the electron-glass phase of this system. The implications of our findings on the slow dynamics of Anderson insulators are discussed. In particular, the reason for the absence of a memory dip and the accompanying electron-glass effects in lightly-doped semiconductors emerges as a natural consequence of their weak disorder.

DOI: 10.1103/PhysRevB.95.134203

I. INTRODUCTION

Theoretical considerations anticipating nonequilibrium effects in Anderson-localized systems were described in a number of papers [1–12]. These were based on the interplay between disorder and Coulomb interactions leading to an electron-glass phase.

Over the last few decades there were several experimental studies that seem to give support to these expectations [13–15]. The dynamics that characterizes the approach to equilibrium of these systems is sluggish; relaxation of the excess conductance produced by driving the system far from the equilibrium was observed to persist for many hours in some cases [16]. The long relaxation of the electronic system makes it possible to observe a modulation of the *single-particle* density-of-states (DOS) in field-effect experiments [17]. This feature, called a 'memory dip' (MD), appears as a cusplike minimum in the conductance versus gate voltage. An example is illustrated in the inset to Fig. 1. The memory dip, presumably [5,9] a reflection of an underlying Coulomb gap [20,21], is the identifying feature of intrinsic electron glass [5,6,9,11,22].

To date, a memory dip has been observed in seven different Anderson insulators (listed in Fig. 1). The figure shows an empirical correlation between the typical width Γ of the MD and the carrier concentration N of the material. The list of Anderson insulators that exhibit electron-glass properties include all types of degenerate Fermi systems; n-type semiconductors (Tl_2O_{3-x}, In_xO, In_2O_{3-x}), p-type semiconductors ($GeSb_xTe_y$, GeTe), and a metal (Be).

The systematic dependence of the MD characteristic width on carrier concentration, an *electronic* property, is consistent with the expectation that the phenomenon is intrinsic. Due to lack of screening in the Anderson-insulating phase, Coulomb interaction may be comparable in magnitude to the quenched disorder, and therefore these competing ingredients responsible for glassy behavior are always present in Anderson insulators.

There seem to be more requirements on the material to allow observation of electron-glass effects. Note that all the systems in Fig. 1 are made from materials with carrier-concentration N limited to a range $10^{22}\ \mathrm{cm}^{-3} > N \geqslant 5\times10^{19}\ \mathrm{cm}^{-3}$. The absence of systems with $N > 10^{22}\ \mathrm{cm}^{-3}$ from this list is not surprising; a prerequisite for observing electron-glass effects is Anderson localization, which is hard to achieve in a system with large N unless by making it granular (on which we remark later). Less clear is the limit of low carrier concentration. No memory dip has been reported in a system with carrier concentration smaller than $\approx10^{19}\ \mathrm{cm}^{-3}$ in any Anderson-localized system like Si or GaAs. Two-dimensional samples of these materials may be tuned to show insulating behavior and were extensively studied in the hopping regime. Their near-equilibrium transport properties (like conductivity versus temperature) are not qualitatively different than those of the systems in Fig. 1. The absence of a MD in these systems has been a vexing question for quite some time.

It was conjectured [22] that relaxation processes in lightly-doped semiconductors (with $N \leqslant 10^{17}\ \mathrm{cm}^{-3}$) are too fast to allow their signature to be captured by field-effect measurements. This was inspired by the observation of relaxation dynamics in a series of amorphous indium-oxide (In_xO) films [22,23]. These can be fabricated with different N values, covering $N \approx 5\times10^{18}\ \mathrm{cm}^{-3}$ to $N \approx 5\times10^{21}\ \mathrm{cm}^{-3}$ by controlling the In-O ratio [24]. The typical relaxation times of these films sharply diminished [23] once the carrier concentration was reduced below $N \approx 10^{20}\ \mathrm{cm}^{-3}$. Note that, given the sample-gate capacitance (as well as the other parasitic circuit capacitances), the field-effect temporal resolution is severely limited for high resistance samples. Consistent with this conjecture, ultrafast relaxation in a lightly-doped semiconductor was reported in phosphorous-doped Si [25]. What needs to be clarified is the role of carrier concentration in affecting the dynamics of electron glasses.

A phenomenon that is highly sensitive to the value of N is often indicative of a many-body mechanism playing a role. Mechanisms that were considered in this regard include correlated many-particle transitions [26] and the Anderson orthogonality catastrophe [27]. A model by Leggett *et al.*, based on coupling to an electronic bath [28], is consistent with many of the observed features [27]. These mechanisms, in conjunction with quenched disorder and hierarchical constraints,

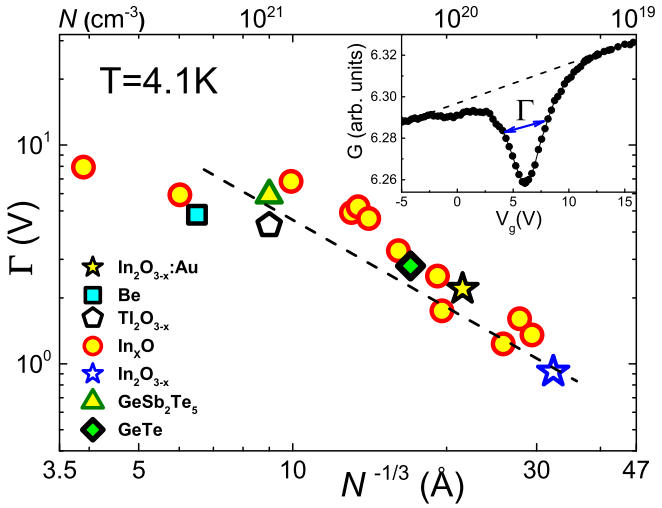

FIG. 1. The typical width of the memory dip Γ as a function of carrier concentration N for several Anderson insulators. Γ is defined in the inset as the width at half height of the dip relative to the thermodynamic G(V_g). Data are taken from Refs. [18,19]. Inset: Field-effect measurement for amorphous indium-oxide film with $N \approx 3\times10^{20}$ cm^{-3} revealing a memory dip centered at +6 V, which is the gate voltage maintained between the sample and the gate for 24 hours before sweeping the gate voltage over the range shown. The In_xO was separated from the gate by 0.5 μm of SiO_2 (the Γ versus N results in the main figure are all normalized to this geometry). The dashed line depicts the law: $\Gamma \propto N^{-1/3}$ which is consistent with the Coulomb-gap behavior suggested by the models in Refs. [5] and [9].

are likely contributing factors in the sluggish relaxation to some degree. However, to account for relaxation times of the order of hours with these scenarios still requires that the *bare* tunneling probabilities are much smaller than those involved in the dc conductivity.

The purpose of this work is to investigate the role played by disorder in slowing down charge rearrangement processes involved in the energy relaxation of electron glasses. This is motivated by an alternative interpretation of the decisive role that seems to be played by the carrier concentration of the system. Note that, at the transition, the magnitude of disorder in an Anderson insulator with large carrier concentration must be larger than that of a system with low carrier concentration, which may be summarized by a simple relation between the Fermi energy of the system and the critical disorder. It will be shown in this paper that this remains true deep into the insulating regime. Therefore, the empirical observation that the relaxation becomes slower once N becomes larger may turn out to be related to the weaker disorder rather than to various many-body effects (although the latter may be quite effective in further slowing down the relaxation).

The first step in examining this conjecture calls for assessing the magnitude of the disorder in the Anderson-insulating phase and its relation to the carrier concentration of the system. We describe a set of experiments on several batches of amorphous indium oxide with different carrier concentrations and with a different degree of disorder in each batch. These data are analyzed to demonstrate a simple relation between disorder and the Fermi energy of a batch with a given N deep into the insulating regime. This, augmented by further arguments, is used to explain why Anderson-localized systems with low carrier concentrations are unlikely to exhibit intrinsic electron-glass effects with relaxation times longer than a few seconds. To understand the motivation for our approach to the problem, we first review the main experimental findings pertinent to the electron-glass dynamics.

A. Basic features of the dynamics in glassy Anderson insulators

Due to the lack of a concrete timescale in their temporal relaxation (generally, a power law), dynamics of glasses cannot be uniquely quantified. Tests to study, on a *relative* basis, how various agents affect the dynamics were performed on Anderson insulating crystalline indium oxide, In_2O_{3-x} and on In_xO with various compositions [23,27,29]. These studies were also limited to effectively two-dimensional (2D) samples with sheet resistances $R_\square$ in the range of ≈1 MΩ to ≈500 MΩ where the signal to noise of the glassy features is favorable. With these systems however, it was possible to test dynamics over a large range of lateral dimensions, from 2 μm to 10 mm [30].

The first observation, already alluded to above, is that dynamics seem to become faster when the carrier concentration is smaller [23]. Secondly, all features associated with slow dynamics disappear as the system crosses over to the diffusive regime [22].

Over the temperature range ≈2–8 K there was no indication of dynamics freezeout [27,29]. This is in stark contrast with the behavior of classical glasses where dynamics is quickly frozen below a certain temperature [31]. The sample conductance over this temperature range typically changes by 1–2 orders of magnitude.

Transition rates associated with conductivity of Anderson insulators can be expressed as: $\omega \exp[-r/\xi]$ were r is the hopping length and ξ the localization length. These rates typically range between $\approx 10^{10}$ sec^{-1} to $\approx 10^{5}$ sec^{-1} based on the transition probability through a bottle-neck resistor with $r/\xi \approx$ 6–15 (a typical value for the hopping regime) and assuming attempt frequency ω of the order of 10^{12} sec^{-1} which is commonly used as the prefactor in hopping conductivity. Here r is the hopping length and ξ the localization length. Relaxation rates of the studied electron glasses are obviously slower by many orders of magnitude.

Another demonstration that conductance and relaxation processes appear to be different was recently observed in photoconductivity experiments on $GeSb_xTe_y$ films in their glassy regime; adding charge to the system by optical excitation enhanced the conductance but it *slowed down* the relaxation dynamics [32].

These observations suggest that relaxation and conductivity involve different processes. It is natural then to consider *extrinsic* effects as a viable mechanism for the slow relaxation exhibited by these systems. There are several candidates to choose from: ion motion, surface traps, grain boundaries [33], and negative-U centers [34] are all potential sources for slow dynamics. Their coupling to charge carriers might be the reason for the observed conductance relaxation observed in the experiments. In the first place, this would immediately explain why relaxation from an out-of-equilibrium state is

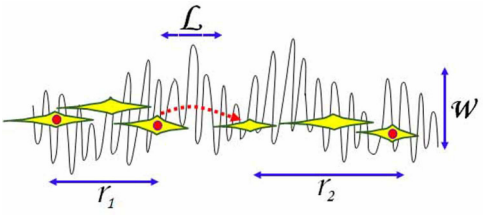

FIG. 2. A schematic description of a proposed element of the asymptotic energy-relaxation process. Charge carriers (full circles) tunneling through potential fluctuations ($\mathcal{W}$) to lower the configurational energy associated with the interparticle Coulomb interaction.

controlled by different processes than those involved in the dc conductance. It is also appealing as a source of a very slow phenomenon, intimately connected with the ubiquitous 1/f-noise phenomenon [35].

This however, is one of the problems with extrinsic mechanisms; flicker noise is indeed ubiquitous; intrinsic electron glassiness is *not*. 1/f noise may be observed in the metallic as well as in the localized transport regime while the electron glass is an *exclusive property of the localized phase*. Furthermore, as mentioned above, a memory dip, which is the identifying feature of the intrinsic electron glass, has not been seen in *any* lightly-doped semiconductors while 1/f noise is quite evident in all these systems. GaAs samples in particular exhibit prominent 1/f noise yet no slow conductance relaxation that might have compromised their operation as bolometers has been observed [36].

Other shortcomings of extrinsic scenarios include difficulties to account for the dependence of the memory dip on temperature and disorder [22]; they cannot explain the systematic dependence of the memory dip width on carrier concentration (Fig. 1), and they cannot account for the peculiar evolution of the MD shape with temperature [22,31]. Finally, the failure of lightly-doped semiconductors to show a memory dip remains enigmatic in this approach.

A more promising route to pursue is the 'purely' electronic scenario which accounts for most of the observed features [5,9–11], and as argued below, the reason for the absence of intrinsic glass effects in low carrier-concentration systems emerges naturally from this picture. In this approach, both conductivity and relaxation in the electron glass proceed via charge-carriers transitions between localized states. The qualitative difference between transitions involved in relaxation and those that control conductivity is that conductance must include activated processes while relaxation, in our scenario, is dominated by tunneling between states differing in energy by $\delta \ll k_B T$ [27].

The driving force for the relaxation is minimizing the electrostatic energy $E_{el} = \sum_{i,j} \frac{e^2}{r_{i,j}\varepsilon(r_{i,j})}$ under the constraints set by the disorder (assumed to be quenched). A simple example of an energy-reducing event due to charge rearrangement is illustrated in Fig. 2.

A transition of the type shown in Fig. 2, for example, would result in an energy release of the order of $\delta\varepsilon = \frac{e^2(r_2-r_1)}{\varepsilon(r_{1,2})r_1 r_2}$ that amounts to a substantial excess energy injected into the system (except for a rare $r_2 \approx r_1$ event). This may enhance the excess conductivity via two possible mechanisms:

First, by generating an excess of nonequilibrium phonons. Although some of these generated phonons would escape to the bath, it does not take much overheating to appreciably affect the conductivity in this regime. Consider for example, a typical electron glass with $R_\square \approx 10$ MΩ at $T = 4$ K. This, when excited, will have an excess conductance ΔG/G of the order of ≈1% (see, e.g., Fig. 6 in Ref. [37]). Overheating by ≈5 mK's (at 4 K) is enough to generate this excess conductance given the R(T) of such a sample (stretched exponential with a power of 1/3 or 1/2 with activation energies of ≈5000 K and 800 K for the indium oxide and Be sample [37], respectively). Even much less overheating will be needed deeper in the electron glass regime; ΔG/G increases algebraically with disorder but the sensitivity of G to temperature increases exponentially with it.

Secondly, a transition event at any point R_i in the system may induce transitions in another site R_j either directly via Coulomb interaction (when $|R_i\text{-}R_j| < r_h$) or indirectly via a succession of 'avalanches' (for $|R_i\text{-}R_j| > r_h$) [38,39] where r_h is the hopping length. As alluded to above, there is no metallic screening in the Anderson-localized phase but at finite temperatures the Coulomb interaction is effectively cut off at distances larger than the hopping length [38,39]. These avalanches, much like the domino effect, ultimately spread to modulate the space-energy configuration of the CCN thus affecting the measured conductance. Relaxation of the excess conductance would last as long as such energy-reducing transitions occur. It should be noted that the probability of these transitions to occur depends also on the electron-phonon coupling strength (direct electron-electron inelastic transitions are essentially suppressed in the strongly-localized system relative to its value in the diffusive regime [38]).

There is also a quantitative difference between transitions involved in the dc conductance and those contributing to relaxation processes. Conductance is determined by relatively fast transitions between a pair of sites composing the current-carrying-network (CCN). These are the pairs of sites connected by the relatively high transition probabilities in the Miller-Abrahams conductance distribution. In the hopping regime the CCN typically occupies a tiny fraction of the system volume; most of the material is 'dead wood:' These are the high resistance regions of the system [40–42], and this is naturally where the slowest transitions occur. Energy relaxation in the Anderson insulator involves energy-reducing transitions anywhere in the system including in particular the dead-wood regions.

The relative weight of the dead wood gains in prominence when the disorder gets larger or when the temperature gets smaller. In our conjecture, this would account for the experimentally observed increase of the relative magnitude of the MD resistance whether affected by disorder, field, or temperature [43].

The dead wood, occupying the bulk of the system volume, holds most of the excess energy associated with the out-of-equilibrium state. Therefore, conductance relaxation in this picture is essentially controlled by the dead-wood slow dynamics.

B. Dynamics in the dead wood

The question we need to address concerns the transition rates of tunneling events of the general type illustrated in Fig. 2.

Tunneling probability depends exponentially on the distance $\mathcal{L}$ and on an effective barrier V^*. Tunneling distance $\mathcal{L}$ for electrons could easily be much larger than that typically found for ions and may extend over 10^2–10^3 atoms in solids. This balances out their transition rates as compared with ions with their $\approx 10^4$ times heavier mass. Tunneling probability may be vanishingly small if $\mathcal{L}$ is long enough. However, the most likely transition scale at the asymptotic regime of the relaxation is perhaps of the order of the Bohr radius a_B. Transitions over longer distances likely proceed by a series of short events. Such 'serial' events, as well as other 'hierarchical processes,' would further slow down the dynamics and should be treated separately.

The quantum transmission through a slab of an Anderson insulator of a finite cross section and length has been worked out by Nikolić and Dragomirova [44]. They studied the statistics of the associated eigenvalues as a function of disorder and for several lengths. The distribution of transmission eigenvalues was found to be very wide. In the presence of moderate disorder it included a finite portion of near resonance channels which may play a role in local hierarchical processes, but they do not directly contribute to relaxation. On the other hand, the distribution of transmission probability was heavily skewed in favor of low transmission channels [43] even for weak disorder while the resonances naturally disappeared when critical disorder was imposed. It is plausible that including electron-electron interaction in such calculations will only enhance the peak of the low transition probabilities in the spectrum. Slow relaxation events should therefore be abundant in the system.

Tunneling probability γ through a simple (square) barrier may be estimated by a WKB expression:

$$\gamma \propto \exp\left(-2\left[\frac{2m^*V^*}{\hbar^2}\right]^{1/2}\mathcal{L}\right); V^* = V - E, \qquad (1)$$

where m^* is the effective-mass of the charge carrier, V the barrier height, and E the particle energy (which will be taken as E_F). The spatial form of $\mathcal{W}(\mathbf{r})$ in a realistic Anderson insulator obviously requires a more elaborate treatment than addressed by the WKB approximation (probably a numerical work along the lines of Ref. [44]). However, the exponential dependence on m^*, $\mathcal{L}$, and V^* should still be reflected in a more detailed treatment. This was recently demonstrated in a numerical study extending the calculations of Ref. [44]; in the localized regime, the probability to find transmission trajectory with a value smaller than a given γ is exponential with $\mathcal{W}^{1/2}$ and $\mathcal{L}$ [45].

To estimate how slow a typical tunneling event may be, one needs to know the magnitude of the V^*. We shall assume it to be of the order of the potential fluctuation $\mathcal{W}$. The value of $\mathcal{W}$ is the distinguishing factor in determining whether electron-glass effects can be observed by field-effect measurements in a given system. $\mathcal{W}$ may vary by orders of magnitudes while a_B is typically in the range of 20–50 Å. Larger values for a_B are usually due to very light effective mass which counteracts the effect of longer tunneling distance on the tunneling probability.

To anticipate the discussion below, recall that a prerequisite for electron-glass behavior is Anderson localization, which means that the disorder energy $\mathcal{W}$ has to be comparable with, or larger than, the kinetic energy E_F. All other things being equal, a system with larger carrier concentration must be more disordered to be Anderson localized and thus has larger $\mathcal{W}$. Lightly-doped semiconductors used for hopping conductivity studies have typically $N \leqslant 10^{17}$ cm^{-3}. Their associated Fermi energy (and thus their $\mathcal{W}$) may be too small to sustain slow transitions. At comparable value of resistivity and reduced temperature k_BT/E_F, their disorder is typically *much* weaker than that of hopping systems with $N \geqslant 10^{20}$ cm^{-3}. What transpires from this consideration is the need to know what actually is $\mathcal{W}$ for a given Anderson insulator. An attempt to deal with this elusive issue is our next step.

C. The 'critical' disorder in Anderson insulators

There are several ways to characterize the magnitude of disorder in the Anderson-localized phase. For example, the value of the localization length ξ is, in a way, a measure of disorder. However, determining ξ involves transport measurements at low temperatures where one probes just the CCN thus ignoring the most disordered part of the sample. Another choice is the Ioffe-Regel parameter $k_F\ell$ that may be estimated from Hall effect and resistivity measurements at relatively high temperatures [46]. $k_F\ell$ may be taken as a measure of disorder whenever ρ is dominated by the elastic mean-free-path ℓ. This condition is well-obeyed in the vicinity of $k_F\ell \simeq 1$ where the conductivity is scale independent [47] and the estimate of $k_F\ell$ is then least sensitive to the specific temperature at which ρ is measured. In the regime $k_F\ell < 1$ neither k_F nor ℓ have their usual meaning but $k_F\ell$ may still be a useful parameter to characterize disorder; it is just a dimensionless parameter that decreases monotonically with disorder. On the other hand, $k_F\ell$ is not simply related to static disorder once $k_F\ell \lll 1$ (or $k_F\ell \gg 1$, a regime irrelevant for this discussion anyhow). In these limiting cases the room-temperature conductivity may be dominated by inelastic processes rather than by static disorder.

Given a system with a certain $k_F\ell$ one still requires a way to assign a value for its $\mathcal{W}$. Theoretical estimates may be used for the 'critical disorder' $\mathcal{W}_\mathcal{C}$, the disorder necessary to just localize the entire band. Estimates based on a noninteracting picture yield the ratio $\mathcal{W}_\mathcal{C}/I \simeq 16.5$ [48]. Here I is of the order of the bandwidth, typically several electron volts. In these models the Fermi energy is taken at midband where the density of states is highest. The models however are more vague when the Fermi energy is near the band edge where $\partial n/\partial\mu$ may be rather small. Unfortunately, this is invariably the situation in real Anderson insulators [48]. It is certainly the case for each of the seven electron glasses listed in Fig. 1.

A more helpful approach then is to rely on the physics of the diffusive regime and extrapolate to the transition point defined by the value of $k_F\ell$ at the transition to the localized phase obtainable from experiments. A measure of disorder for a diffusive system is $\mathcal{W} = \hbar/\tau$ where τ is the transport mean-free-time.

On the metallic side the ratio $\frac{\hbar/\tau}{E_F} = \frac{2}{k_F\ell}$, so at the metal-insulator transition:

$$\mathcal{W}_\mathcal{C} = \beta E_F, \qquad (2)$$

where β depends on the specific value of $(k_F\ell)_c$—the Ioffe-Regel parameter evaluated at the transition to the

localized phase:

$$\beta = \frac{2}{(k_F \ell)_c}. \quad (3)$$

The experiments described next, suggest that the proportionality between E_F and $\mathcal{W}$ is still valid deep into the insulating regime ($k_F \ell \ll 1$), covering the entire range of resistances probed in the electron-glass studies.

D. Gauging disorder by monitoring optical properties; tuning disorder in the amorphous indium oxides

A system that allows a continuous tuning of disorder for both sides of the metal insulator is amorphous indium oxide In_xO. It may also be prepared with a vastly different carrier concentration (between $\approx 5\times10^{18}$ cm^{-3} and $\approx 6\times10^{21}$ cm^{-3}) by controlling the In/O ratio. This makes it possible to study the dependence of the electron-glass properties on carrier concentration and disorder [24], as well as the metal insulator [24] and the superconductor-insulator transition [49].

The feasibility of tuning the system resistivity by heat treatment is a rather unique trait of In_xO. It is possible to vary the room-temperature resistance of the as-prepared In_xO sample by up to five orders of magnitude while maintaining its amorphous structure and composition (and hence carrier concentration). A before-and-after diffraction pattern illustrating the preservation of amorphicity in the heat treatment is shown in Fig. 3. This figure demonstrates that the amorphous structure remains intact during thermal annealing. Actually, one is hard pressed to see a difference in the before-and-after diffraction patterns (Fig. 3). It takes a careful measurement of the diffraction-ring intensity profile to discern the difference; a narrowing of the diffraction rings, as shown in Fig. 4. The change in the resistance is essentially due to modified mobility; Hall effect studies showed only a small change as a result of the annealing process [46,50]. It was also found that the material volume decreases during the process which could be detected by measuring the thickness of the film for example, by x-ray interferometry as demonstrated in Fig. 5.

This result was part of an extensive work designed to measure the change in the optical properties that accompany the thermal annealing of In_xO samples [46] with different carrier concentrations. We bring here fuller results and interpretation of these data.

The volume change caused by annealing the sample was reflected in the absorption versus energy plot as a reduction of the optical gap. This is illustrated in Fig. 6 for one of the studied batches.

The dependence of absorption coefficient $\alpha(\omega)$ on energy ω of all our In_xO samples obeys the relation:

$$\alpha(\omega)\hbar\omega = B(\hbar\omega\text{-}E_g). \quad (4)$$

A volume reduction that occurs concomitantly with a smaller optical gap is often observed in pressure studies of amorphous materials [51–53]. The increase in wave functions overlap due to the reduced volume leads to a wider bandwidth and to a modified $\partial n/\partial\mu(E)$. A schematic of such a change in the conduction-band shape is depicted in Fig. 7. Note that this depiction is consistent with the observed

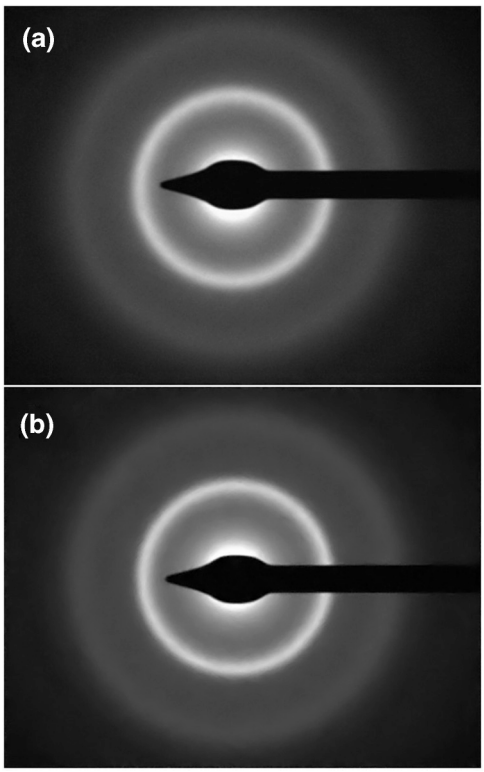

FIG. 3. Electron diffraction patterns (using a 200 kV beam) of a $\approx$50 nm In_xO film for the as-prepared specimen with sheet resistance $R_\square > 10^8$ Ω (a) and after thermal annealing for 34 days yielding $R_\square \approx 7\times10^4$ Ω (b). The general appearance of the pattern seems unchanged in the annealing, but a careful comparison of the strong diffraction ring between the (a) and (b) micrographs reveals slightly less fuzziness in the annealed sample (illustrated in Fig. 4 below).

before-and-after absorption curves and with the sum rule of the number of states. However, it does not into account for a modification in the valence band and should only be viewed as a pedagogical aid. This modification of the band shape

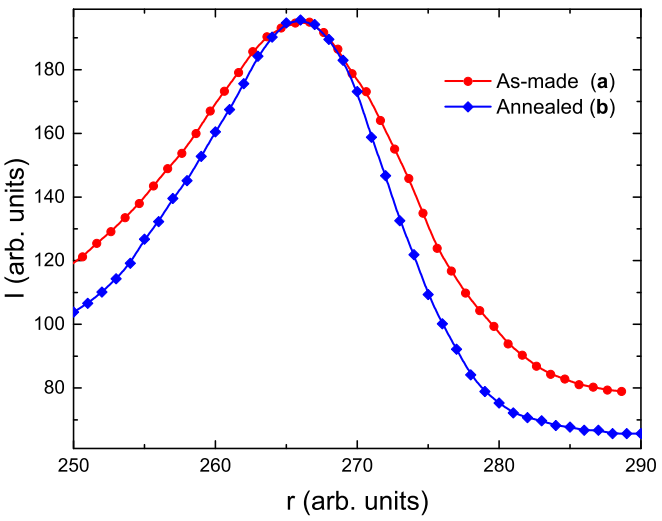

FIG. 4. Intensity profile of the strongest rings in the diffraction pattern of both (a) and (b) micrographs shown in Fig. 3 as a function of distance r from the diffraction center. Data were taken by averaging line scans using imagej.

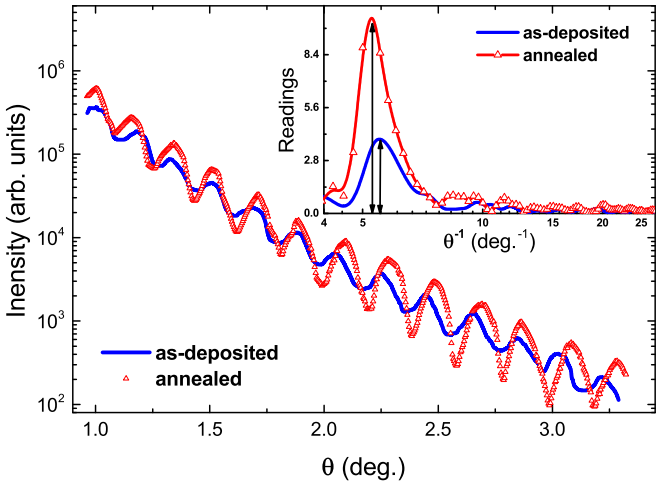

FIG. 5. Reflection interferometry using a Cu Kα x-ray source (wavelength = 1.54 Å) for the before-after annealing stages of a similar film as in Fig. 3. The inset shows the Fourier transform of the main plot exposing both the reduced film thickness in the annealed sample and the enhanced visibility of the interference pattern.

is a more plausible explanation for the reduced optical gap in the thermal-annealing experiments than the effect of the mobility-edge shift offered in Ref. [46]. The similarity in the effects produced by applying hydrostatic pressure [51–53] and thermally annealing the sample is not surprising; in both cases energy is supplied to a metastable system allowing it to cross barriers associated with its being a structural glass.

Our study includes a detailed comparison of the optical properties with simultaneously measured changes of the disorder parameter $k_F\ell$. The values for $k_F\ell$ and the Fermi energy E_F used here are based on free-electron formulas $E_F = \frac{\hbar^2(3\pi^2 N)^{3/2}}{2m^*}$ and $k_F\ell = (3\pi^2)^{2/3}\hbar\sigma_{RT}/e^2N^{1/3}$, where σ_{RT} is the conductivity (measured at room temperature) and m^* is the effective mass.

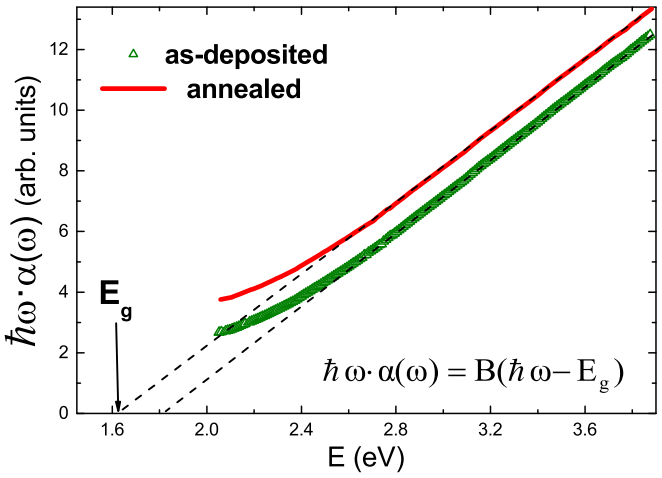

FIG. 6. Absorption versus photon energy for a before-and-after In_xO sample (characterized by carrier concentration $N \simeq 8.5\times10^{19}$ cm^{-3}). Dashed lines delineate the respective values of the energy gap.

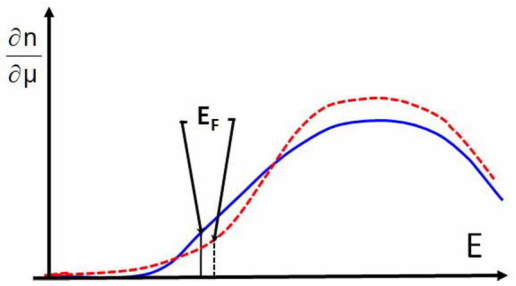

FIG. 7. A schematic depiction of the conduction-band shape for the as-prepared (dashed line) and annealed (full line) specimen. This assumes that the change in the valence band may be neglected. Note that $\partial n/\partial\mu$ at E_F may actually increase during the thermal annealing due to the combined effect of reduced Lifshitz-tail and midband widening.

Both optical and electrical measurements were performed *in situ* on thick (900–1100 Å), effectively 3D films of In_xO. Data for the optical gap E_g were collected at intermediate stages of the annealing process starting from the as-prepared sample with typically $k_F\ell \leqslant 10^{-3}$ and ending in $k_F\ell > 1$. The process was repeated with films of various carrier concentrations. Figure 8 shows the dependence of E_g on $k_F\ell$ for each of the studied samples.

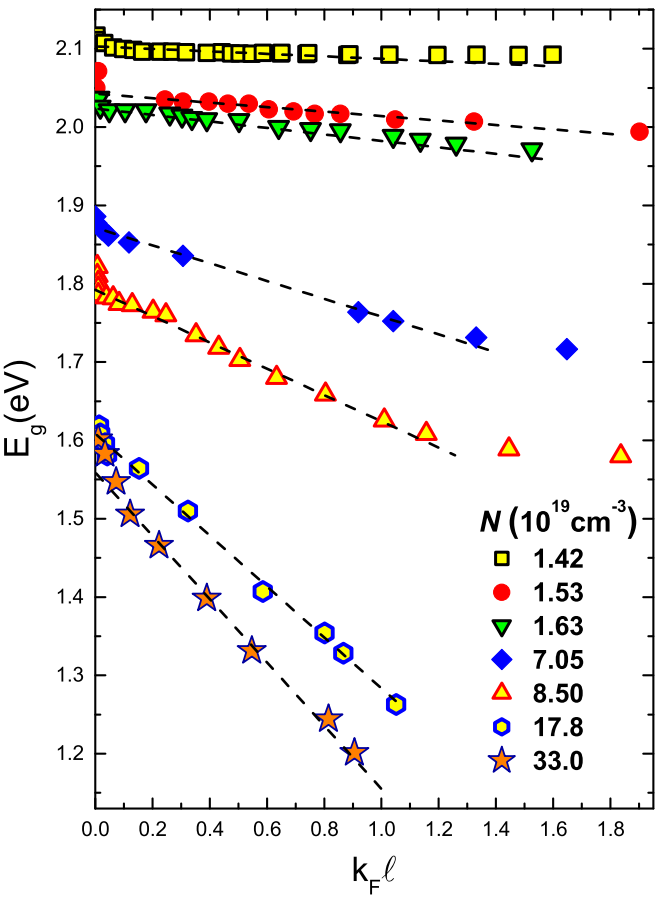

FIG. 8. The dependence of the optical gap E_g on the Ioffe-Regel $k_F\ell$ parameter for the seven batches (labeled by their respective N) of In_xO samples. Dashed lines are guides to the eye.

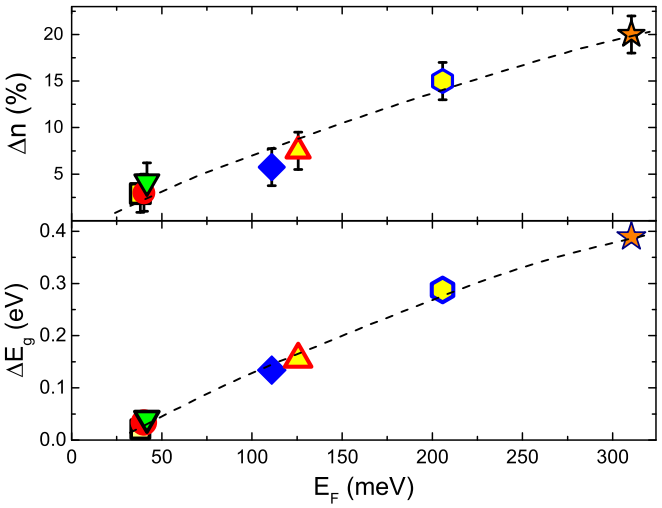

FIG. 9. ΔE_g and Δn are the respective changes in the optical gap E_g and the refractive index n when the disorder is changed (by thermal annealing) from $k_F\ell \approx 0.02$ to $k_F\ell = 1$. The data points stand for each of the batches studied (labeled by symbols corresponding to each of the batches in Fig. 8).

The systematic trend that emerges here is that the optical gap E_g is a monotonous function of $k_F\ell$ or rather, both $k_F\ell$ and E_g depend monotonically on the sample volume. Secondly, for a given change in $k_F\ell$, the concomitant change in E_g depends on the carrier concentration N of the batch; ΔE_g is bigger for the batch with the larger N. The change of the refractive index n (judged by the change in the prefactor B in Eq. (3) [54]) during the annealing process showed a similar trend. Figure 9 shows a systematic correlation between E_F and the change in disorder of n and E_g for each of the batches studied (for a unity change in $k_F\ell$).

II. ANALYSIS AND DISCUSSION

Before proceeding it may be a good idea to check whether our assumptions so far are not at odds with reality. We have focused on In_xO because of available data pertaining to this system with a wide range of carrier concentration and disorder. In particular, the metal-insulator transition has been studied in this material for In_xO versions with $N \simeq 10^{19}$ cm^{-3} and $N \simeq 10^{21}$ cm^{-3}. Both versions were found to cross the transition at a similar $k_F\ell \simeq 0.32 \pm 0.02$ [24]. To localize In_xO with $E_F \approx 0.3$ eV, which is the highest Fermi energy in the series studied here, $\mathcal{W}_C$ has to be $\gtrsim$1.9 eV [to be consistent with Eq. (3)]. Is such disorder a viable occurrence in this system?

A main source of disorder in In_xO is chemical [24,46]. This is associated with deviation from stoichiometry; relative to the ionic compound In_2O_{3-x}, there are 5–30% oxygen vacancies in In_xO [24]. To preserve chemical neutrality some of the indium atoms must assume a valence of +1 instead of the +3 they have in the stoichiometric compound. When randomly distributed these valence fluctuations form a background potential of $e^2/r \approx 5$ eV (assuming an average interatomic separation of $r \approx 3$ Å [55]). This type of disorder is quite prevalent in nonstoichiometric compounds, metallic oxides, high-Tc materials, etc. The associated disorder $\mathcal{W}$ in these materials may reach 4–5 eV.

In addition to chemical disorder, there is an *off-diagonal* disorder in the material that is partially alleviated in the thermal annealing process. This disorder is related to the distributed nature of the interatomic separation (the random values of interatomic separation). The distribution of interparticle distances (and thus wave-function overlap) obviously gets narrower as the volume decreases and the system approaches the 'ideal' closed-packed amorphous structure. The diminishment of this, off-diagonal disorder, is clearly reflected in the enhanced visibility of the x-ray interference pattern of the annealed sample in Fig. 4 and also in the electron diffraction Figs. 3 and 4 (albeit less conspicuously).

It has been a controversial issue whether off-diagonal disorder can lead to localization [56–58]. It should be noted that, in the In_xO system, the metal-insulator transition is crossed by the combined effect of changing the atomic overlap (which in turn affects the density of states as schematically described in Fig. 6) while simultaneously modifying the off-diagonal disorder. Localization (at the less-annealed regime) is also aided by the underlying chemical disorder and possibly by the Coulomb interaction [59].

Two features of the data in Figs. 7 and 8 are worth noticing: First, for a given batch (fixed N) there is a systematic and monotonous dependence of E_g on $k_F\ell$ although the transport measures essentially just the elements of the CCN while optics is sensitive to the whole sample. The correlation between the two measurements is indicative of an underlying common conductance distribution; being disordered the system is inherently inhomogeneous but it is so in a generic way (as embodied in the percolation treatment of hopping conductivity). Inhomogeneity associated with large thickness or composition variations across the sample will in general not show the correlation between transport and a bulk measurement. Secondly, the change in both the optical gap and the refractive index between $k_F\ell = 1$ and $k_F\ell \simeq 0$ exhibits a near-linear correlation with the Fermi energy of each batch (Figs. 8 and 9).

As noted above, during annealing the sample volume decreases (Fig. 5), which among other things, causes the refractive index to increase. Δn may then be used to estimate the associated change in the system energy per particle δE. Let us take the largest swing of Δn in the series being $\approx$20% for the sample with $E_F \simeq 300$ meV (Fig. 8). The average change of the interparticle separation in this case is $\approx$7% (an estimate consistent with the thickness change upon annealing measured independently for this sample) giving $\delta E \approx 0.07 \times 5$ eV $= 350$ meV. Note that this energy is close to the respective change of the optical gap for this batch (Fig. 8). The near linearity of Δn and ΔE_g with E_F guarantees that proportional results are obtained for the entire series of samples studied here. This means that the disorder energy in the range $k_F\ell = 1$ to $k_F\ell = 0$ changes by no more than E_F of the batch under study.

For the electron-glass phase of In_xO however the relevant range of $k_F\ell$ is only $0 < k_F\ell < 0.32$; In_xO sample with $k_F\ell \approx 0.02$ has a resistance of $\approx$1 GΩ at 4 K [24], therefore the change in δE is even smaller than E_F. The entire change of disorder relevant for the electron-glass phase of In_xO can be concisely summarized as $\delta E \lesssim \beta' E_F$ where $\beta' \approx 0.3$. This

can be combined with Eq. (2) to give a measure of the disorder W_{EG} in the electron-glass regime (namely, deep in the Anderson-localized phase):

$$\mathcal{W}_{EG} \approx (\beta + \beta')E_F = \beta^* E_F. \quad (5)$$

Most of the disorder in $\mathcal{W}_{EG}$ is actually due to $\mathcal{W}_C = \beta E_F$. An order of magnitude estimate for $\mathcal{W}$ in the diffusive regime may be taken as $\mathcal{W} = \hbar/\tau = \hbar V_F/\ell$ (τ is the transport mean-free time). With $E_F = \hbar^2 k_F^2/2m^*$ this yields for the ratio $\mathcal{W}/E_F = 2/k_F\ell$. As the transition of In_xO is approached from the diffusive regime $k_F\ell \to 0.32$ and $\mathcal{W} \to \mathcal{W}_C \approx 6.2E_F$. Increasing the disorder above this point further localizes the system, but as the resistance is exponential with disorder in this regime, a relatively small added amount of disorder $\approx 0.3E_F$ is necessary to get deep ($k_F\ell \lll 1$) into the insulating state.

The near-linear relation between disorder and Fermi energy established here for In_xO samples is significant; these samples cover more than a decade range in carrier concentration and over this range the dynamics is changing by almost three orders of magnitude [23]. This is a result of the exponential dependence of relaxation dynamics on $\mathcal{W}_{EG}$ as is argued next. Our conjecture is that a relation between $\mathcal{W}$ and E_F of the form expressed by Eq. (5) and with $\beta^*$of similar magnitude as in In_xO is generally obeyed by Anderson insulators.

If lightly-doped semiconductors follow the same trend, their dynamics should be much faster than in electron glasses with $N \geqslant 3\times10^{20}$ cm^{-3}. To illustrate, let us use Eq. (1) on a relative basis to compare the typical tunneling probability for the In_xO sample with $N \approx 3.3\times10^{20}$ cm^{-3} with that of a lightly-doped semiconductor like Si. Equation (1) with $m^* \approx 0.3m_0$, $V^* \approx 1.7$–1.9 eV, and $\mathcal{L} \approx 20$ Å gives $\gamma \approx 10^{-7}$. The parameters for Si-MOSFET in the Anderson insulating regime [60] are similar except for V^*; given a carrier concentration of $N \approx 10^{17}$cm^{-3}, typical of the insulating phase in this system [60], E_F is $\approx$100 times smaller. Since β^* is likely only smaller when the Fermi energy is reduced [48], the respective $\mathcal{W}$ for Si should be at least two orders of magnitude smaller than that of the In_xO sample, which means five to six orders of magnitude faster dynamics (assuming comparable electron-phonon coupling strength and a similar spectral nature of the disorder). If conductance relaxation in the In_xO may be observed for days, it may not last more than seconds in a lightly-doped semiconductor like Si. With such a relaxation time it would be practically impossible to observe the memory dip in field-effect experiments. It is hard to see how any parameter peculiar to a lightly-doped semiconductor can compensate for their weak disorder. Note that the estimate made above is just for the *bare* tunneling, it does not take into account coupling to the environment, which would further increase the discrepancy between these rates [27].

A test of these considerations is to instill a disorder of few electron volts in a lightly-doped semiconductor: By our conjecture, slow relaxation and intrinsic electron-glass effects should be observable in this case. Unfortunately, the measurement of such a sample may turn out to be a tall order. With such strong disorder ($W/E_F \ggg 1$) it is doubtful whether the conductance is measurable even at temperatures that exceed the Fermi energy while, like in any other electron glass, one should maintain $T \ll E_F/k_B$ in such a measurement, which

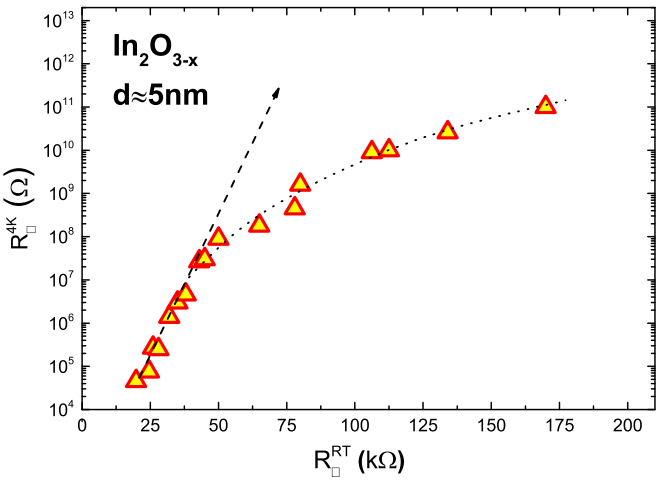

FIG. 10. The sheet resistance of a In_2O_{3-x} film at $T = 4.1$ K versus its value at room temperature. The dashed line depicts the expected value of resistance extrapolated along the line where the room-temperature resistance may be a linear measure of disorder. The dotted curve is a guide for the eye.

for these systems means $T \ll 1$ K. At these temperatures the resistance for a sample with such W will balloon out of reach.

The difficulty can be demonstrated by reference to an experiment using as a model a thin film of In_2O_{3-x}, a system where the resistance can be manipulated over a considerable range. In the experiment, shown in Fig. 10, the room-temperature resistance R_{RT} of the In_2O_{3-x} film is changed by UV treatment [50].

Samples with R_{RT} spanning the range of $\approx$16–180 kΩ were generated from a single batch in this method. At T $\approx$ 4.1 K these samples had resistances spanning $\approx$6 orders of magnitude. The value of R_{RT} may be taken as a (linear) measure of disorder only when the sample is in the diffusive regime, $R_{RT} \lesssim h/e^2$. Strong-localization behavior apparently sets in for $R_{RT} \gtrsim 40$ kΩ where the linear relation between disorder and R_{RT} does not hold. Over the range of $R_{RT} = 16$–32 kΩ, a mere factor of $\approx$2 in disorder, the resistance at 4.1 K changes by $\approx$4 orders of magnitude. By extrapolation from the regime where R_{RT} is a linear measure of disorder, changing it by an order of magnitude would increase the resistance (at $\approx$4 K) by $\approx$20 orders of magnitude, yielding a resistance that defies current measurements techniques. We suspect that similar catastrophe would occur upon cranking up the disorder in lightly-doped semiconductors.

A more feasible test is a low-temperature study of a weakly-localized system ($k_F\ell \gg 1$). This can be realized for instance by using a two-dimensional (2D) film of In_2O_{3-x} which has been extensively studied in the weakly-localized regime. Being 2D, the system should crossover to the strongly-localized regime [61] at sufficiently low temperature despite having *sub-critical* disorder (in the 3D sense). At sufficiently low temperatures its resistance could be as high as a sample with $k_F\ell \ll 1$ of this material that exhibits glassy effects at say $\approx$4 K [15,22,27]. The logic presented above anticipates that the weakly-disordered sample would exhibit at best very weak memory dip in field-effect experiments (it may not show a null

effect due to occasional regions with potential fluctuation of large amplitude).

It should be emphasized that by itself, large resistance does not guarantee electron glassiness; resistance may result from many factors not related to the type of disorder discussed here. For example, regions of hard gaps such as a series inclusion of band-insulator or isolated islands of superconductivity in the current path [24] may exhibit huge resistances without necessarily showing glassy effects on extended time scales.

Another corollary of the proposed picture is that relaxation times cannot be arbitrarily long. This is a result of the maximum value of $\mathcal{W}$ available in reality. Naturally occurring defects in condensed matter systems have an energy of the order of bandwidths, which limits their ability to Anderson localize a system. Indeed, to localize a typical metal with Fermi energy of ≈3–4 eV, one has to mix it with another material, usually a band insulator, rendering the system granular.

Some of the electron-glass transport features are exhibited by granular systems in their activated regime. In particular, they show a memory dip and slow relaxation [62]. The element of the relaxation in the granular systems, common with the electron glass, is re-distribution of charges in space to lower the 'electrostatic' energy of the system. Their dynamics however is expected to be different than that of Anderson insulators; charge re-distribution between different grains is probably controlled by Coulomb blockade constraints. Charging energies of typical grains could be quite large, which may lead to extremely long relaxation times. This was demonstrated by the Bar-Ilan group; in their experiments on several granular systems it was shown that below a few degrees Kelvin dynamics became so slow that it was impossible to follow the evolution of a memory dip [63]. The constraints posed by charging energies may be partially alleviated by random fields in the insulating matrix in which the metallic granules are embedded but then the dynamics is controlled by extrinsic elements. These issues deserve further study.

In summary, the empirical attributes of the electron-glass dynamics lead us to conclude that a significant part of the slow relaxation observed in systems with relatively large carrier concentration has to do with their much stronger disorder. The elements of the relaxation process are assumed to be tunneling events that proceed to ultimately minimize the system energy under the constraints of disorder and Coulomb interaction. The slowest transitions naturally occur in the dead-wood regions of the system that in the hopping regime occupy most of the system volume. Slow 'fluctuators' are abundant in these regions even for a rather short tunneling distance once the disorder is appreciable. An estimate of the disorder energy $\mathcal{W}$ for a realistic sample that shows electron-glass properties was made using In_xO as a model system. This was based on measurements of the metal-insulator transition made on these compounds, free-electron concepts, and on optical data relevant for their strongly-disordered regime. It was shown that $\mathcal{W}$ is proportional to the Fermi energy of the Anderson-insulating system for the entire range of disorder relevant for the electron-glass measurements. All other things being equal, and given the exponential dependence of the tunneling rate on $\mathcal{W}$, one expects energy relaxation in lightly-doped semiconductors where E_F is two orders of magnitude smaller, to be many orders of magnitude faster as indeed established experimentally [25].

There is still the challenge of accounting for the protracted relaxation times observed in the experiments. This is a problem common to all glasses, but the flexibility of experimenting with electron glasses seems to offer more scope for progress. From the theory point of view the problem has proved to be difficult; even when a complete knowledge of the disorder is at hand there are other pieces of the puzzle that need careful elaboration. In particular, coupling to the environment may play a role in further slowing-down transition rates. Environmental degrees of freedom that follow adiabatically the tunneling object would modify the transition rate through mass enhancement (polaronic effects). More generally, coupling to the environment will suppress tunneling due to the Anderson orthogonality catastrophe (AOC) [27]. Recent work focused on new aspects of the AOC (originally conceived for clean systems [64]) in the strongly-localized and interacting regime [65,66]. However, a model incorporating coupling to the environment for a medium lacking screening (like an Anderson-insulator), is more pertinent for our experiments. To our knowledge, this aspect has not been adequately addressed by any work so far. Other effects that probably contribute to slow relaxation are hierarchical constraints (the 'domino' effect being a special case) and correlated many-electron transitions. Fundamental questions related to these scenarios are yet to be resolved. However, to understand why a memory dip is not likely to be observed in lightly-doped semiconductors by transport measurements, it may suffice to consider just the role of disorder.

ACKNOWLEDGMENTS

The author gratefully acknowledges illuminating discussions with Eldad Bettelheim and Ori Grossman and for sharing insight based on their numerical study. This research has been supported by Grant No. 1126/12 administered by the Israel Academy for Sciences and Humanities.

[1] J. H. Davies, P. A. Lee, and T. M. Rice, Phys. Rev. Lett. **49**, 758 (1982); M. Grünewald, B. Pohlman, L. Schweitzer, and D. Würtz, J. Phys. C **15**, L1153 (1982).

[2] J. H. Davies, P. A. Lee, and T. M. Rice, Phys. Rev. B **29**, 4260 (1984).

[3] M. Pollak and M. Ortuño, Sol. Energy Mater. **8**, 81 (1982); M. Pollak, Phil. Mag. B **50**, 265 (1984).

[4] G. Vignale, Phys. Rev. B **36**, 8192 (1987).

[5] C. C. Yu, Phys. Rev. Lett. **82**, 4074 (1999).

[6] M. Müller and L. B. Ioffe, Phys. Rev. Lett. **93**, 256403 (2004).

[7] V. Malik and D. Kumar, Phys. Rev. B **69**, 153103 (2004).

[8] R. Grempel, Europhys. Lett. **66**, 854 (2004); A. B. Kolton, D. R. Grempel, and D. Dominguez, Phys. Rev. B **71**, 024206 (2005).

[9] E. Lebanon and M. Müller, Phys. Rev. B **72**, 174202 (2005); M. Müller and E. Lebanon, J. Phys. IV France **131**, 167 (2005).

[10] A. Amir, Y. Oreg, and Y. Imry, Phys. Rev. B **77**, 165207 (2008); Annu. Rev. Condens. Matter Phys. **2**, 235 (2011).

[11] Y. Meroz, Y. Oreg, and Y. Imry, Europhys. Lett. **105**, 37010 (2014).

[12] M. Pollak, M. Ortuño, and A. Frydman, *The Electron Glass* (Cambridge University Press, England, 2013).

[13] M. Ben-Chorin, D. Kowal, and Z. Ovadyahu, Phys. Rev. B **44**, 3420 (1991).

[14] M. Ben-Chorin, Z. Ovadyahu, and M. Pollak, Phys. Rev. B **48**, 15025 (1993).

[15] A. Vaknin, Z. Ovadyahu, and M. Pollak, Phys. Rev. B **65**, 134208 (2002).

[16] Z. Ovadyahu, Phys. Rev. B **73**, 214204 (2006).

[17] The field effect, much like the Hall effect is usually conceived as a thermodynamic measurement and then it is $\partial n/\partial \mu$ that it is probed not the single-particle density of states. The situation is different when the gate is scanned with a rate that is faster than the relaxation time of the electronic system.

[18] Z. Ovadyahu, Phys. Rev. B **88**, 085106 (2013).

[19] Z. Ovadyahu, Phys. Rev. B **94**, 155151 (2016).

[20] M. Pollak, Discuss. Faraday Soc. **50**, 13 (1970); G. Srinivasan, Phys. Rev. B **4**, 2581 (1971).

[21] A. L. Efros and B. I. Shklovskii, J. Phys. C: Solid State Phys. **8**, L49 (1975).

[22] Z. Ovadyahu, Phys. Rev. B **78**, 195120 (2008).

[23] A. Vaknin, Z. Ovadyahu, and M. Pollak, Phys. Rev. Lett. **81**, 669 (1998).

[24] U. Givan and Z. Ovadyahu, Phys. Rev. B **86**, 165101 (2012).

[25] V. K. Thorsmølle and N. P. Armitage, Phys. Rev. Lett. **105**, 086601 (2010).

[26] J. Matulewski, S. D. Baranovskii, and P. Thomas, Phys. Status Solidi **5**, 694 (2008), and references therein.

[27] Z. Ovadyahu, Phys. Rev. Lett. **99**, 226603 (2007).

[28] A. J. Leggett, S. Chakravarty, A. T. Dorsey, M. P. A. Fisher, A. Garg, and W. Zwerger, Rev. Mod. Phys. **59**, 1 (1987).

[29] Z. Ovadyahu, Phys. Rev. B **73**, 214208 (2006).

[30] V. Orlyanchik and Z. Ovadyahu, Phys. Rev. B **75**, 174205 (2007).

[31] C. A. Angell, J. Non-Cryst. Solids **131**, 13 (1991), and references therein.

[32] Z. Ovadyahu, Phys. Rev. Lett. **115**, 046601 (2015).

[33] V. I. Kozub, Y. M. Galperin, V. Vinokur, and A. L. Burin, Phys. Rev. B **78**, 132201 (2008), and references therein.

[34] P. W. Anderson, Phys. Rev. Lett. **34**, 953 (1974); J. Phys. Colloques **37**, 339 (1976).

[35] P. Dutta and P. M. Horn, Rev. Mod. Phys. **53**, 497 (1981); M. B. Weissman, *ibid.* **60**, 537 (1988).

[36] D. McCammon, M. Galeazzi, D. Liu, W. T. Sanders, B. Smith, P. Tan, K. R. Boyce, R. Brekosky, J. D. Gygax, R. Kelley, D. B. Mott, F. S. Porter, C. K. Stahle, C. M. Stahle, and A. E. Szymkowiak, Phys. Stat. Sol. (B) **230**, 197 (2002).

[37] Z. Ovadyahu, Y. M. Xiong, and P. W. Adams, Phys. Rev. B **82**, 195404 (2010).

[38] Z. Ovadyahu, Phys. Rev. Lett. **108**, 156602 (2012); Phys. Rev. B **91**, 035113 (2015).

[39] M. Palassini and M. Goethe, J. Phys.: Conf. Ser. **376**, 012009 (2012).

[40] B. I. Shklovskii and A. L. Efros, Sov. Phys. JETP **33**, 468 (1971).

[41] V. Ambegaokar, B. I. Halperin, and J. S. Langer, Phys. Rev. B **4**, 2612 (1971).

[42] M. Pollak, J. Non-Cryst. Solids **11**, 1 (1972); K. Mallory, Phys. Rev. B **47**, 7819 (1993).

[43] This trend has been consistently observed in each and every system that exhibited the memory dip.

[44] Nikolić and Dragomirova, Phys. Rev. B **71**, 045308 (2005).

[45] O. Grossman and E. Bettelheim (unpublished).

[46] Z. Ovadyahu, Phys. Rev. B **47**, 6161 (1993).

[47] Y. lmry, Phys. Rev. Lett. **44**, 469 (1980).

[48] B. R. Bulka, B. Kramer, and A. MacKinnon, Z. Phys. B: Condens. Matter **60**, 13 (1985); B. Bulka, M. Schreiber, and B. Kramer, *ibid.* **66**, 21 (1987).

[49] D. Shahar and Z. Ovadyahu, Phys. Rev. B **46**, 10917 (1992).

[50] Z. Ovadyahu, J. Phys. C: Solid State Phys. **19**, 5187 (1986).

[51] W. Fuhsp, Schlotter, and J. Stuee, Phys. Stat. Sol. (B) **57**, 587 (1973).

[52] S. Onari, T. Inokuma, H. Kataura, and T. Arai, Phys. Rev. B **35**, 4373 (1987).

[53] K. Miyauchi, J. Qiu, M. Shojiya, Y. Kawamoto, and N. Kitamura, J. Non-Cryst. Solids **279**, 186 (2001).

[54] M. Zavetova and B. Velicky, in *Optical Properties of Solids*, edited by B. O. Seraphin (North-Holland, Amsterdam, 1976).

[55] J. Rosen and O. Warschkow, Phys. Rev. B **80**, 115215 (2009).

[56] E. N. Economou and P. D. Antoniou, Solid State Commun. **21**, 285 (1977).

[57] J. Stein and U. Krey, Z. Phys. B **34**, 287 (1979).

[58] T. Odagaki, Solid State Commun. **33**, 861 (1980).

[59] M. Amini, V. E. Kravtsov, and M. Müller, New J. Phys. **16**, 015022 (2014).

[60] S. V. Kravchenko, G. V. Kravchenko, J. E. Furneaux, V. M. Pudalov, and M. D'Iorio, Phys. Rev. B **50**, 8039 (1994).

[61] Z. Ovadyahu and Y. Imry, J. Phys. C **16**, L471 (1983).

[62] C. J. Adkins, J. D. Benjamin, J. M. D. Thomas, J. W. Gardner, and A. J. McGeown, J. Phys. C: Solid State Phys. **17**, 4633 (1984); G. Martinez-Arizala, D. E. Grupp, C. Christiansen, A. M. Mack, N. Markovic, Y. Seguchi, and A. M. Goldman, Phys. Rev. Lett. **78**, 1130 (1997); G. Martinez-Arizala, C. Christiansen, D. E. Grupp, N. Marković, A. M. Mack, and A. M. Goldman, Phys. Rev. B **57**, R670(R) (1998); T. Grenet, Eur. Phys. J **32**, 275 (2003); N. Kurzweil and A. Frydman, *ibid.* **75**, 020202 (2007).

[63] T. Havdala, A. Eisenbach, and A. Frydman, Europhys. Lett. **98**, 67006 (2012).

[64] P. W. Anderson, Phys. Rev. Lett. **18**, 1049 (1967).

[65] D.-L. Deng, J. H. Pixley, X. Li, and S. D. Sarma, Phys. Rev. B **92**, 220201(R) (2015).

[66] V. Khemani, R. Nandkishore, and S. L. Sondhi, Nat. Phys. **11**, 560 (2015).